

Trajectory Generation using Sharpness Continuous Dubins-like Paths with Applications in Control of Heavy Duty Vehicles

Rui Oliveira^{1,2}, Pedro F. Lima^{1,2}, Marcello Cirillo², Jonas Mårtensson¹ and Bo Wahlberg¹

Abstract— We present a trajectory generation framework for control of wheeled vehicles under steering actuator constraints. The motivation is smooth autonomous driving of heavy vehicles. The key idea is to take into account rate, and additionally, torque limitations of the steering actuator directly. Previous methods only take into account curvature rate limitations, which deal indirectly with steering rate limitations. We propose the new concept of Sharpness Continuous curves, which uses cubic and sigmoid curvature trajectories together with circular arcs to steer the vehicle. The obtained trajectories are characterized by a smooth and continuously differentiable steering angle profile. These trajectories provide low-level controllers with reference signals which are easier to track, resulting in improved performance. The smoothness of the obtained steering profiles also results in increased passenger comfort. The method is characterized by a fast computation time, which can be further speeded up through the use of simple pre-computations. We detail possible path planning applications of the method, and conduct simulations that show its advantages and real time capabilities.

I. INTRODUCTION

A. Background and Motivation

Path planning deals with the generation of paths or trajectories (paths with an associated time law) for a vehicle. The generated paths/trajectories are then used as a reference signal for the controllers implemented in the vehicle. Planning methods for autonomous vehicles have come a long way from the initial problem of finding collision free paths, being now focused on properties such as kinodynamic constraints, optimality, and uncertainty [1], [2]. Non-holonomic systems, such as car-like vehicles, must follow specific patterns of motion, that are defined by their kinematic constraints. These constraints introduce an additional difficulty, as they limit the maneuverability of the vehicle, resulting in limited types of paths that are admissible, *i.e.*, can be feasibly followed.

Steering methods are planners that are able to compute a path between vehicle states in an environment without obstacles. Even though the vast majority of autonomous vehicle applications involve the presence of obstacles, steering methods still prove to be useful, as they are often used as part of obstacle avoiding path planners [3]–[6].

The Dubins path [7] is a steering method able to connect two arbitrary vehicle poses through a minimal length path.

*This work was partially supported by the Wallenberg Autonomous Systems and Software Program (WASP)

¹School of Electrical Engineering, ACCESS Linnaeus Centre, KTH Royal Institute of Technology, SE-100 44 Stockholm, Sweden
rfoli@kth.se, pfrdal@kth.se, jonas1@kth.se, bo@kth.se

²Scania, Autonomous Transport Solutions, Södertälje, Sweden
marcello.cirillo@scania.com

However it is limited to vehicles moving either forward or backward and assumes instantaneous changes in the angular velocity. This concept was later extended to a vehicle that is able to change directions along the path, *i.e.* switch between forward and backward motion, resulting in the Reeds-Shepp paths [8].

Both [7] and [8] assume instantaneous angular velocity changes, resulting in paths with a discontinuous curvature profile. To perfectly track these paths, a car-like vehicle would have to immediately change its steering angle, or alternatively, to steer while stopped, which is not feasible/desirable in practice.

In order to achieve curvature continuous paths, [9] proposed an extension to Reeds-Sheeps paths. Making use of clothoidal paths, the authors developed a steering method that provides curvature continuous paths. Clothoids are an obvious choice, since they have long been used in road design, as they allow for smooth driving [10]. Additionally the curvature and curvature rate are bounded, making them more suitable to be followed by actual car-like vehicles.

Curvature continuity is, however, not enough for path feasibility. The continuity must also be present in the sharpness, that is, the curvature rate. A discontinuity in the sharpness of the path implies an infinite acceleration in the steering wheel actuator, that renders the path impossible to track precisely. Sharpness continuity, and consequently path feasibility, are thus, of extreme importance when precise maneuvering is needed. In such case, we would like to provide the vehicle with paths that are easy to follow [11]. By generating references that are easier to follow, the low-level controller performance is expected to improve. Passenger comfort comes as an added benefit, due to the smoother curvature profiles imposed by a continuous sharpness.

To the best of our knowledge, [12] is the only work addressing sharpness continuity. However, the method only takes into account the curvature and sharpness of the path, not tackling the actual steering actuator limitations.

B. Main Contributions

The contribution of this work comes from the generation of vehicle trajectories that:

- Directly take into account steering actuator magnitude, rate, and torque limitations;
- Ease the controller task and improve passenger comfort;
- Can connect arbitrary poses with arbitrary curvatures;
- Have fast computation times.

We build upon the work of [9], replacing clothoidal paths with cubic and sigmoid curvature paths. Cubic curvature

paths are easy and intuitive to compute. Even though they are only differentiable, instead of infinitely differentiable, as in [12], they still result in paths which do not require infeasible torques from a steering wheel actuator. Sigmoid curvature paths take inspiration from [12], and they are used due to their characteristic smooth profile. Additionally, we formulate the constraints so that we can limit the actual steering angle rate and steering angle acceleration of the vehicle, instead of the sharpness of the path, as done in previous approaches [9], [12]. The maximum steering angle rate and acceleration are more intuitive constraints than the maximum sharpness, and they can be directly obtained from the vehicle actuator limitations. The proposed method is also computationally inexpensive and can be used as part of an online planner in autonomous vehicle systems.

C. Outline

The structure of the paper is as follows. In Section II, we present the vehicle model used and the problem to be solved. Following that, Section III presents the proposed method to solve the stated problem. Sections IV and V present Cubic Curvature and Sigmoid curvature paths, which are used to construct sharpness continuous paths. Section VI contains experimental simulation results, showcasing the performance of the method. Some conclusions and directions of future work are presented in Section VII.

II. PROBLEM STATEMENT

A. Vehicle Model

We start by defining the vehicle model as:

$$\begin{pmatrix} \dot{x} \\ \dot{y} \\ \dot{\theta} \\ \dot{\kappa} \end{pmatrix} = \begin{pmatrix} \cos \theta \\ \sin \theta \\ \kappa \\ 0 \end{pmatrix} v + \begin{pmatrix} 0 \\ 0 \\ 0 \\ 1 \end{pmatrix} \sigma.$$

(x, y) represents the location of the vehicle rear wheel axle center and θ its orientation. The curvature κ of a vehicle with wheelbase length l is related to its steering angle ϕ through

$$\kappa = \frac{\tan \phi}{l}. \quad (1)$$

The steering angle of the vehicle is set by an actuator, which like any real system has physical limitations. The limitations we target in this work are:

- Maximum steering angle amplitude ϕ_{max} ,
- Maximum steering angle rate of change $\dot{\phi}_{max}$,
- Maximum steering actuation acceleration $\ddot{\phi}_{max}$.

These limitations effectively affect the vehicles motion capabilities and should be dealt with when generating paths to be followed.

B. Path Feasibility

Path feasibility depends on the capabilities of the vehicle that performs it and on the path itself. The limited steering angle amplitude ϕ_{max} imposes a maximum allowed curvature on the path κ_{max} . By generating paths which have a curvature profile $|\kappa| \leq \kappa_{max}$, as done by Dubins [7], it is

possible to address this limitation. Limited steering angle rate of change $\dot{\phi}_{max}$ is tackled in [9] by limiting the sharpness of the generated paths.

In this paper, we deal with the third limitation, related to the limited steering angle acceleration $\ddot{\phi}_{max}$. Having a limited $\dot{\phi}_{max}$ results in ϕ being a continuous function, which in turn indicates that ϕ is a continuously differentiable, \mathbf{C}^1 function. The paths generated by [9] have corresponding $\dot{\phi}$ profiles with discontinuities, that require an infinite $\ddot{\phi}_{max}$. This is impossible to achieve by an actuator, and motivates the usage of paths with a \mathbf{C}^1 steering profile.

The steering profile is related to the curvature profile through (1). The sharpness α is defined as the spatial derivative of the curvature

$$\alpha = \frac{\partial \kappa}{\partial s},$$

where s is the distance along the path. By ensuring sharpness continuity in a path, we guarantee that the curvature, and the steering profile of such a path is \mathbf{C}^1 , and that a vehicle will be able to follow it with bounded steering acceleration $\dot{\phi}_{max}$.

In the following section, we detail how to generate paths that respect all three limitations previously stated.

III. SHARPNESS CONTINUOUS PATHS

A. Principle

Dubins paths use a combination of arc circle turns and/or line segments to connect two arbitrary poses. The arc circle turns have a turning radius of κ_{max} guaranteeing that a maximum steering angle ϕ_{max} is never exceeded. In [9], this idea is extended with so called Curvature Continuous (CC) turns, which replace arc circles by a combination of clothoid and arc circle segments so as to guarantee curvature continuity.

We extend this idea further, replacing the clothoid segments by cubic and sigmoid curvature paths, and in that way, achieving sharpness continuity. This comes with the added benefit that such paths are feasible with a limited steering acceleration $\ddot{\phi}_{max}$.

B. Sharpness Continuous Turns

We propose a novel concept of a turn, called Sharpness Continuous (SC) turn. Unlike the previously proposed CC turns [9], an SC turn is able to achieve curvature rate continuity.

The SC turn consists of three segments, an initial cubic or sigmoid curvature path Γ_a , a circular arc Γ_o , and a final cubic or sigmoid curvature path Γ_b . Figure 1 shows an example of a SC turn. The initial segment Γ_a starts at a configuration \mathbf{q}_a and ends with maximum curvature, $\pm \kappa_{max}$. The second segment is a circular arc Γ_o with radius κ_{max}^{-1} and arbitrary arc length. The SC turn is completed with a path Γ_b , with starting curvature $\pm \kappa_{max}$ and ending at a configuration \mathbf{q}_b .

We assume, without loss of generality, that the vehicle, and subsequently the path, starts at a configuration $\mathbf{q}_a = (x_a, y_a, \theta_a, \kappa_a) = (0, 0, 0, 0)$. From \mathbf{q}_a , it then follows the path Γ_a taking it to a configuration $\mathbf{q}_i = (x_i, y_i, \theta_i, \kappa_{max})$.

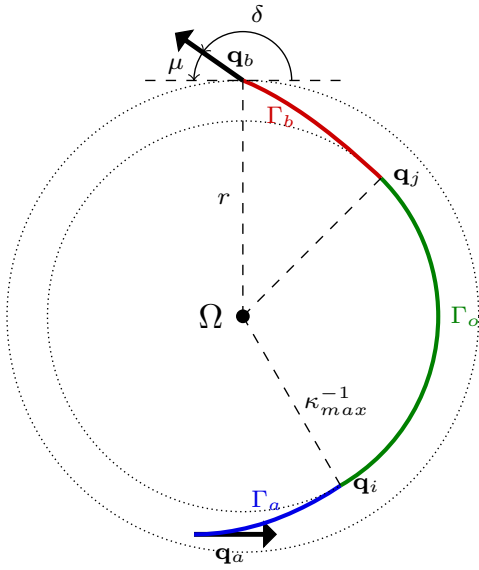


Fig. 1: Sharpness continuous turn general case

The path has as initial and final conditions $\kappa_i = \kappa_a$ and $\kappa_f = \kappa_{max}$. The values x_i , y_i , and θ_i are those that result from following the curvature profile of Γ_a with a starting vehicle state \mathbf{q}_a .

Once the vehicle has a curvature κ_{max} , it then follows a circular arc path $\Gamma_ο$ with radius κ_{max}^{-1} . The circular arc starts at the position (x_i, y_i) and has its center at a distance κ_{max}^{-1} perpendicular to the orientation θ_i from point (x_i, y_i) . The center is then given by

$$(x_\Omega, y_\Omega) = (x_i - \kappa_{max}^{-1} \sin \theta_i, y_i + \kappa_{max}^{-1} \cos \theta_i). \quad (2)$$

The last path segment Γ_b departs from the circular arc and it brings the vehicle to a configuration $\mathbf{q}_b = (x_b, y_b, \theta_b, \kappa_b)$. Configuration \mathbf{q}_b depends on the point of departure from the circular arc, \mathbf{q}_j . However, it always lies in a circle Ω , which has the same center as the circular arc, (x_Ω, y_Ω) .

In order to find the radius of circle Ω , we first assume an auxiliary circular arc to be centered at $(x_{\Omega_z}, y_{\Omega_z}) = (0, \kappa_{max}^{-1})$. We then assume a departure configuration from the circle at $(0, 0, \theta, \kappa_{max})$. Then, by following the path given by a curvature profile with initial and final curvatures $\kappa_i = \kappa_{max}$ and $\kappa_f = \kappa_g$, we will end at a configuration $\mathbf{q}_z = (x_z, y_z, \theta_z, \kappa_z)$. \mathbf{q}_z is a configuration located at an auxiliary Ω_z circle (the auxiliary equivalent of the Ω circle), which has the same center as the circular arc. Thus we can compute the radius of Ω_z , which is equal to the radius of Ω , as

$$r = \sqrt{(x_g - x_{\Omega_z})^2 + (y_g - y_{\Omega_z})^2} = \sqrt{x_g^2 + (y_g - \kappa_{max}^{-1})^2}. \quad (3)$$

An additional angle μ is defined as being the difference between θ_b and the tangential angle to Ω at configuration \mathbf{q}_b . It is computed using the previous auxiliary circular arc as

$$\mu = \arctan\left(\frac{y_b - \kappa_{max}^{-1}}{x_b}\right) + \frac{\pi}{2} - \theta_b \quad (4)$$

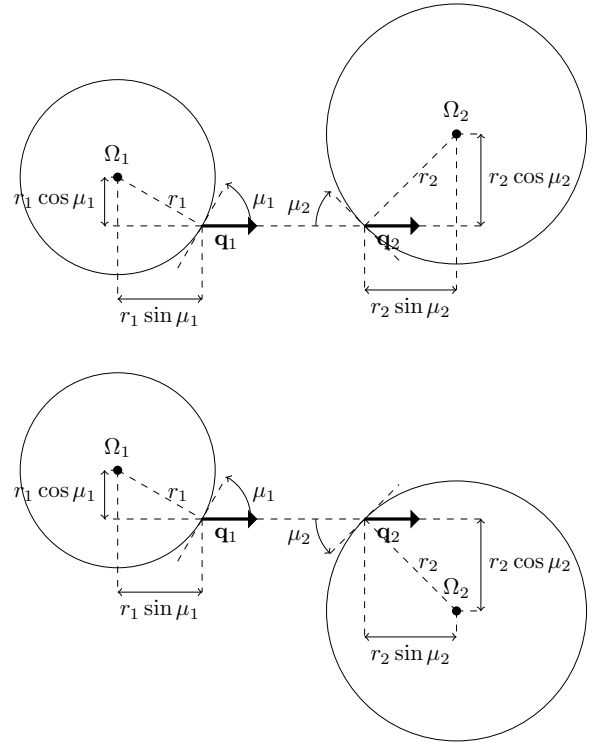


Fig. 2: Computing the external (top) and internal (bottom) tangents

It can then be observed that given a certain initial configuration \mathbf{q}_a , the possible positions of the ending configuration \mathbf{q}_b , resulting from a combination of a cubic or sigmoid curvature path, a circular arc, and another cubic or sigmoid curvature path lie on a circle Ω . The possible θ_b orientations of these configurations are given by the tangential angle at the circle plus μ .

C. Connecting Sharpness Continuous Turns

A SC path between start and goal configurations \mathbf{q}_s and \mathbf{q}_g can be found by connecting two SC turns. Such path consists of three elements:

- a SC turn starting at the initial configuration \mathbf{q}_s and ending at a configuration with null curvature \mathbf{q}_1 ,
- a line segment starting at \mathbf{q}_1 and ending at \mathbf{q}_2 , with orientation equal to both \mathbf{q}_1 and \mathbf{q}_2 ,
- a SC turn starting at configuration \mathbf{q}_2 with null curvature, and ending at the final configuration \mathbf{q}_g .

In order to connect two SC turns, we need to find the configurations \mathbf{q}_1 and \mathbf{q}_2 that belong to the starting and ending SC turn possible departure configurations, and that can be connected with a line segment. That is, \mathbf{q}_1 and \mathbf{q}_2 must have the same orientation θ , and both must lie on a line segment with an inclination angle θ .

As seen before, the possible set of departure configurations of a SC turn are located in a circle, and its orientations differ from the circle tangent by μ . Thus, to connect two SC turns, we need a way to connect two circles Ω_s and Ω_f with arbitrary centers, radii, and μ values.

We first assume two auxiliary circles Ω_1 and Ω_2 , as depicted in Figure 2 (top). Ω_1 and Ω_2 have the same radii and μ values as the original circles Ω_s and Ω_f . Ω_1 is centered at $(0, 0)$ and Ω_2 is located so that \mathbf{q}_1 and \mathbf{q}_2 are collinear. We are interested in finding the center of $\Omega_2 = (x_{\Omega_2}, y_{\Omega_2})$. From Figure 2 (top) it can be seen that

$$y_{\Omega_2} = -r_1 \cos \mu_1 + r_2 \cos \mu_2. \quad (5)$$

We assume that the distance $r(\Omega_1, \Omega_2)$ between the circle centers is the same as the distance of the original circles $r(\Omega_s, \Omega_f)$. We then have

$$x_{\Omega_2} = \sqrt{r(\Omega_s, \Omega_f)^2 - y_{\Omega_2}^2}. \quad (6)$$

We know that $\mathbf{q}_1 = (r_1 \sin \mu_1, -r_1 \cos \mu_1, 0)$ and $\mathbf{q}_2 = (x_{\Omega_2} - r_2 \sin \mu_2, y_{\Omega_2} - r_2 \cos \mu_2, 0)$. In order to find these configurations in the original circles Ω_s and Ω_f , we need to first apply a rotation $\Delta_\theta = \arctan(y_{\Omega_g} - y_{\Omega_s}, x_{\Omega_g} - x_{\Omega_s})$ to q_1 and q_2 . We then translate these configurations by $(\Delta_x, \Delta_y) = (x_{\Omega_s}, y_{\Omega_s})$. The resulting rotated and translated configurations correspond to the desired tangent configurations between the circles Ω_s and Ω_f .

The above procedure finds the departure configurations between two counter clockwise (left steering) SC turns (shown in Figure 2 (top)). The same procedure, with minor alterations, can also be used to find the possible departure configurations between any combination of clockwise (right steering) and counter clockwise turns. Figure 2 (bottom) shows an example of counter clockwise and clockwise turns.

This method is valid as long as the found tangent configurations \mathbf{q}_1 and \mathbf{q}_2 do not lie inside the circles Ω_2 and Ω_1 , respectively.

D. Small Orientation Change Turns

A SC turn can sometimes have a very small orientation change δ between its starting and departing poses. Let us define $\delta_\theta(\Gamma_i)$ and $\delta_\theta(\Gamma_f)$ as the orientation changes between the initial and final poses of paths Γ_i and Γ_f . For an orientation change $|\delta| < |\delta_\theta(\Gamma_i) + \delta_\theta(\Gamma_f)|$, the SC turn has to perform a very long circular arc segment, so that it can correctly connect the start pose to the departing pose.

In order to avoid this large turn, the method presented in [9] uses a combination of a clothoid and a symmetric clothoid, that achieves this exact orientation change without having to travel along the arc circle. In [13], the same authors found analytical expressions for this elementary path, that can achieve such an orientation change, and end up at the necessary departure configuration. Unfortunately, in our case we were not able to derive analytical expressions for the case of cubic and sigmoid curvature profiles.

To achieve a SC turn that can achieve a small orientation change δ without having to resort to a large circular arc segment, we make use of splines. In [14], seventh order polynomials are used to generate paths between two arbitrary configurations. Using the same method we connect the starting pose to the departing pose. We additionally enforce a sharpness of zero at the endpoints in order to guarantee sharpness continuity.

E. Finding the Shortest SC Path

In order to find the shortest SC path between two configurations \mathbf{q}_s and \mathbf{q}_g , we need to compute all the possible SC turns that can be spanned from these configurations. The SC turns are then connected, in order to generate possible SC paths. The process is detailed below.

Each of the configurations \mathbf{q}_s and \mathbf{q}_g can span a total of four SC turns, depending if the vehicle is moving forwards or backwards, or if the vehicle is turning left or right. The case of a SC turn which assumes the vehicle moving forward and turning left is shown in Figure 1. The method explained in section III-B can be readily used to obtain SC turns moving forward, independent of the direction they are turning. The procedure to obtain a SC turn moving backwards is fairly similar, the only difference being that now the SC turn is constructed backwards from the desired configuration from which we wish to span the SC turn.

In total, there are 16 possible paths between the two sets of 4 SC turns spanned from configurations \mathbf{q}_s and \mathbf{q}_g . Each path is found by computing the SC path, resulting from connecting two SC turns, as detailed in section III-C. Each SC path length is evaluated, and the shortest of all possible paths is then selected as the solution.

IV. CUBIC CURVATURE PATHS

A. Introduction

Cubic curvature paths are defined as paths with a cubic curvature profile $\kappa(s) = a_3 s^3 + a_2 s^2 + a_1 s + a_0$, where s is the length along the path. As an example, clothoids have instead a linear curvature profile $\kappa(s) = a_1 s + a_0$, where a_1 is the clothoid sharpness α , and a_0 the initial curvature of the clothoid $\kappa(0) = \kappa_i$.

We choose a cubic curvature profile because it is the minimum degree polynomial which allows us to define arbitrary initial and final curvatures, κ_i and κ_f , and sharpnesses α_i and α_f . The sharpness profile of these paths is given by:

$$\alpha(s) = \frac{\partial \kappa(s)}{\partial s} = 3a_3 s^2 + 2a_2 s + a_1. \quad (7)$$

In order to find the parameters of the cubic polynomial, we use the initial and final constraints:

$$\begin{aligned} \kappa(0) &= \kappa_i = a_0, \\ \alpha(0) &= \alpha_i = a_1, \\ \kappa(s_f) &= \kappa_f = a_3 s_f^3 + a_2 s_f^2 + a_1 s_f + a_0, \\ \alpha(s_f) &= \alpha_f = 3a_3 s_f^2 + 2a_2 s_f + a_1, \end{aligned} \quad (8)$$

where s_f is the path length, and is itself an unknown.

In our application we want to ensure sharpness continuity, for this purpose we need to set the initial and final sharpness values, α_i and α_f to zero. This allows us to stitch together cubic curvature paths with other path segments while ensuring sharpness continuity.

B. Ensuring Steering Rate and Acceleration Constraints

In order to have a feasible path, we need to ensure that a vehicle can follow it while complying with its steering limits. By ensuring that both κ_i and κ_f are smaller in magnitude than κ_{max} , we ensure that the cubic curvature path always has a steering angle magnitude smaller than κ_{max} .

The steering angle profile corresponding to the cubic curvature path is first computed from the path curvature using (1). Assuming then that the vehicle is following the path at a given velocity v , the steering angle rate and acceleration profiles are computed. Both profiles have a peak magnitude rate $\dot{\phi}_{peak}$ and acceleration $\ddot{\phi}_{peak}$. In case $\dot{\phi}_{peak}$ is larger than the allowed maximum steering rate $\dot{\phi}_{max}$ the length s_f needs to be increased so that $\dot{\phi}_{peak} = \dot{\phi}_{max}$. This can be achieved by simply scaling the path length by $\dot{\phi}_{peak}/\dot{\phi}_{max}$. Similarly if $\ddot{\phi}_{peak} > \ddot{\phi}_{max}$, we scale the path length, however this time by a scaling factor of $\sqrt{\ddot{\phi}_{peak}/\ddot{\phi}_{max}}$. In order to make sure that the path respects both rate and acceleration limitations, we need to scale its length by the greater of the two scaling factors. Once the new path length s_f is computed, the cubic curvature path is recomputed, by solving the linear equation system given by the initial and final cubic polynomial constraints (8).

V. SIGMOID CURVATURE PATHS

A. Introduction

Sigmoids are comprised of several functions which achieve an "S"-like shape. One such function is the hyperbolic tangent $\tanh(x)$. Paths with a curvature profile given by an hyperbolic tangent slowly change from one curvature to another in a very smooth way.

We consider paths which follow a curvature profile of the type $\kappa(s) = A \tanh(Bs)$, where A depends on the desired initial and final path curvatures, and B is a tunable parameter, controlling the smoothness of the path.

Assuming that $A = 1$, we plot the resulting hyperbolic tangent function for different values of B in Figure 3. It can be seen that an increasing magnitude of B results in a sharper transition. The sharper the transition, the more difficult the curvature profile is to follow. Choosing a too small value of B will result in easy to follow paths, but at the cost of large path lengths.

We want our path to start at an initial curvature κ_i and finish at a final curvature κ_f . Once decided on a certain B value, B^* , we evaluate the function $\kappa(x) = A \tanh(B^*x)$, in the interval $x \in [-1, 1]$. To achieve the desired curvature change between κ_i and κ_f we need

$$A^* = \frac{(\kappa_f - \kappa_i)}{2 \tanh(B^*)}$$

The function $\kappa(x) = A^* \tanh(Bx) - A^* \tanh(-B) + \kappa_i$ will then, in the domain $x \in [-1, 1]$ take values from κ_i to κ_f .

B. Sharpness Discontinuity

The sharpness profile of a sigmoid curvature path is given by

$$\alpha(s) = A^* B \operatorname{sech}^2\left(B\left(s - \frac{s_f}{2}\right)\right),$$

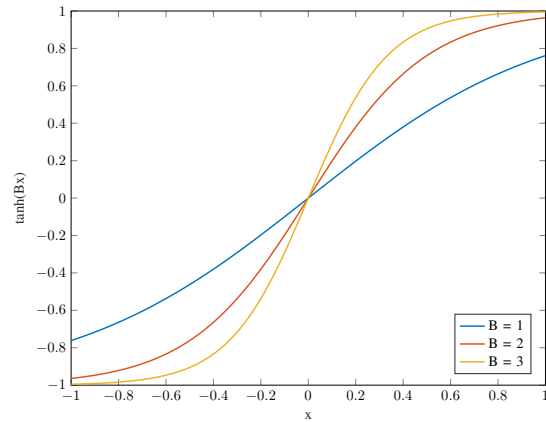


Fig. 3: Influence of B in the hyperbolic tangent function

which at the beginning and ending of the path $s = 0$ and $s = s_f$, has a non-null sharpness $\alpha = \pm A^* B \operatorname{sech}^2\left(B\frac{s_f}{2}\right)$. This means that if we stitch a sigmoid curvature path with another path that has an initial or final null sharpness, we do not have the desired sharpness continuity property. However the magnitude of the discontinuity can be reduced by increasing the magnitude of the B value. By choosing large enough B values, this discontinuity becomes almost unnoticeable.

C. From Maximum Steering Rate to Maximum Sharpness

As for the case of cubic curvature paths, the steering rate and acceleration profiles of the path need to be computed. A scaling of the path length is then performed to ensure that the path complies with the steering rate and acceleration limits. The procedure to do so follows the same steps as explained in IV-B.

VI. RESULTS

A. Convergence of SC Paths to Dubins Paths

As previously mentioned the Dubins paths are proven to be optimal in terms of length. The CC and SC paths are, however, longer than the Dubins path. This happens because the CC and SC turns have longer turning radii than a stand alone circular arc with a radius $r = \kappa_{max}^{-1}$.

In Figure 4, we show the Dubins path for a given start and goal configuration. We then overlay SC paths with different maximum sharpness for the same start and goal configurations. It can be seen that the greater the maximum sharpness of the SC paths is, *i.e.* the greater the achievable steering rate and accelerations of the vehicle, the closer it approaches the Dubins path. This is somewhat intuitive, as increasing the maximum sharpness of the path results in increasing the rate of change of the curvature profile. If $\alpha_{max} \rightarrow \infty$, then the curvature transitions from and to κ_{max} would be immediate, and the SC path would be equivalent to the Dubins path.

B. Notes on Computational Complexity

As previously mentioned, given two configurations \mathbf{q}_s and \mathbf{q}_g , the SC method computes all possible SC turns and how they can be connected. The connection process, as detailed

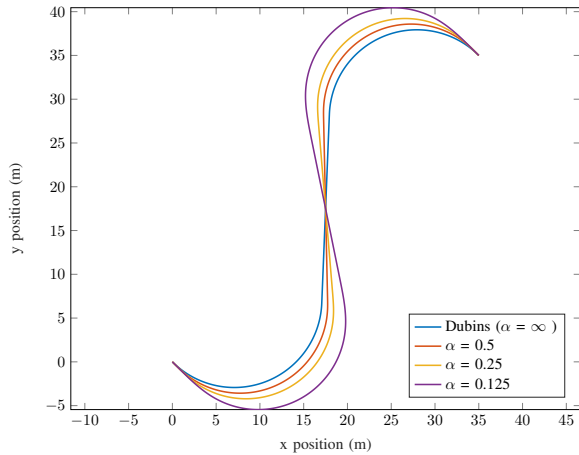


Fig. 4: SC paths with increasing sharpness α converge to the Dubins path

in section III-C, is computationally cheap, requiring only a few trigonometric operations.

The bulk of processing comes from finding the possible SC turns each configuration can span. As seen in section III-B, a SC turn depends on the cubic or sigmoid curvature paths that are part of it. In order to evaluate these paths, one has to generate their curvature profiles from the given initial and final constraints. To comply with the steering constraints, a numerical evaluation of a steering profile must be done, in order to find the path length scaling factors, as detailed in section IV-B. When one has the desired curvature profile, the orientation θ can be obtained analytically. The x and y positions of the path are, however, found by solving the vehicle model equations, using an Euler method. The computational cost of this, results from a trade-off between desired precision and required real-time capabilities of the SC method.

In order to greatly decrease the computation complexity of the method, some shortcuts can be taken, as detailed in the following section.

C. Precomputation of Cubic Curvature Paths

As previously stated, the SC method computation speed is limited by the generation of the cubic or sigmoid curvature paths. Depending on the application however, some assumptions can be made, which can greatly improve the query time of the method, by allowing a precomputation of the cubic or sigmoid curvature paths to be used.

If one assumes that the start and end configurations always have null curvatures, then one can compute in an initialization procedure, all the possible cubic or sigmoid curvature paths starting and ending at curvatures $\kappa = 0, \pm\kappa_{max}$. In this way, we skip the expensive generation of cubic curvature paths needed to find out the possible SC turns, greatly reducing the computation time of the SC method. In order to generate a SC turn, one just has to use the precomputed paths and apply rotations and translations on them.

The precomputation of paths can still be achieved, without limiting the start and goal configurations to have null curva-

ture. In fact, one can allow the start and goal configuration to have curvature values in a discrete set $\mathbb{K} = [\kappa_1, \kappa_2, \dots, \kappa_N]$.

D. Spline Computations

In the case when small turn paths need to be used (detailed in section III-D), a numerical evaluation of the whole spline path is needed. Determining the coefficients of a spline is computationally cheap, but generating the path points is expensive, as it requires a simulation of a vehicle model, in order to find the x and y positions.

Furthermore, splines of such high order, are prone to be numerically unstable, resulting in curvature profiles with a large magnitude. This phenomena becomes more evident the closer the poses are and the smaller the deflection angle is. Thus, after a spline path is computed, an evaluation step is required, in order to check that the path complies with the steering limitations of the vehicle.

E. Timing Evaluation

We test the steering method, measuring its computational speed for several problem instances. The method is implemented in C++ and running on a Linux Mint distribution. The computer used is equipped with an Intel Core i7-6820HQ Processor running at 2.70 GHz, and with 16,0 GB of RAM.

We randomly generate 1000 queries to the steering method. The start and goal configurations of each query are generated by sampling the x and y coordinates from a uniform random distribution between -50 and 50 . The orientations sampled from the interval $[-\pi, \pi]$, and the curvatures are from the discrete equispaced set of curvatures $[-\kappa_{max}, \dots, 0, \dots, \kappa_{max}]$. The set of discrete curvatures has in total 11 elements.

In the first test, we simply evaluate queries resulting in a path that does not require spline computations. For each query that is found to result in an SC path without splines, we run the query first using precomputed paths and then without using the precomputed paths. For each query we compute the resulting SC path 100 times, and average its running time. When making use of precomputations, we get an average time for finding the solution of $70\mu\text{s}$, while without precomputations we get an average time of 12ms . The precomputations prove to be of extreme importance, increasing the computational performance up to 3 orders of magnitude.

The second test follows the previous setup, but now only measuring the performance of SC path solutions that have a spline in it. 1000 queries are evaluated, and averaged over 100 repetitions. When using precomputations, we get an average query time of $100\mu\text{s}$. Without precomputations we get 14ms .

The reported results indicate that the steering method is extremely inexpensive when making use of precomputations. Even in the case when no precomputations are made, the method runs in few milliseconds, making it suitable for real-time applications.

F. Simulations

A simulation test is run in order to understand how do the proposed paths influence the performance of a vehicle tracking them. A kinematic vehicle model coupled with an accurate steering actuator model are used to simulate a heavy duty vehicle.

In the test, three paths consisting of a straight segment, a turn, and a straight segment are generated. The first path is generated as a CC path [9]. The second and third paths, are generated using our proposed SC paths, where the second path uses cubic curvature paths (referred to as SC-Cubic), and the third path uses sigmoid curvature paths (referred to as SC-Sigmoid). All three paths are generated so that they abide by the same maximum steering angle magnitude ϕ_{max} , steering angle rate $\dot{\phi}_{max}$, and steering angle acceleration $\ddot{\phi}_{max}$ constraints. As previously explained, the CC paths require an infinite $\dot{\phi}_{max}$, being so, the CC path only respects the steering magnitude and rate constraints.

The simulation assumes a steering actuator that is limited in terms of achievable steering angle magnitude, rate and acceleration. The steering angle is controlled making use of a tuned PID controller, which receives a steering angle reference, and actuates on the steering angle acceleration. The PID controller was tuned to achieve a satisfactory step response, characterized by a relatively fast settling time and with very little overshoot. The steering angle reference is provided from a high-level controller, which is responsible for tracking the path. The high-level controller consists of a feedforward part and a feedback part. The feedforward part is obtained by finding the closest path point, and getting the corresponding steering angle at that point. The feedback part consists in a proportional controller which tries to regulate both the lateral and heading error. Such a controller is a simple implementation commonly used in path tracking applications.

Figure 5 shows the steering reference profiles of the three paths to be tracked. It can be seen that they consist of two straight segments connected by a turning motion. The difference between them is in the shape of the increasing and decreasing sections of the steering angle. In the CC case, the steering angle change follows a linear profile, in the SC-Cubic it follows a cubic profile, and in the SC-Sigmoid case it follows a sigmoid profile.

Figure 6 shows the measured lateral and heading errors when the vehicle tries to track the different paths. The vehicle is initially placed at the start of the path, and it follows the first straight segment perfectly, as expected. However, when the turning section starts, a deviation from the path begins to arise. This is due to the performance of the low-level PID controller, which is not able to follow the feedforward steering reference exactly, as is expected of a real system. The feedback part is then responsible for trying to regulate the errors to zero.

Shortly after the turn begins the CC path becomes unstable whilst both the SC-Cubic and SC-Sigmoid paths are stable, and their error then tends to zero. The error profiles show

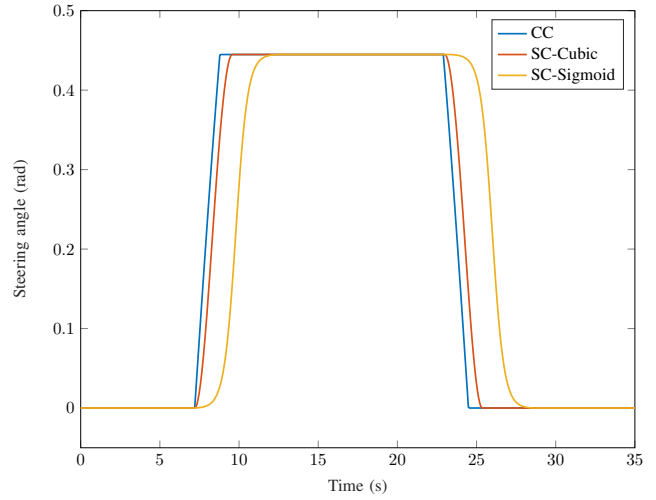


Fig. 5: Steering reference profiles used in simulation

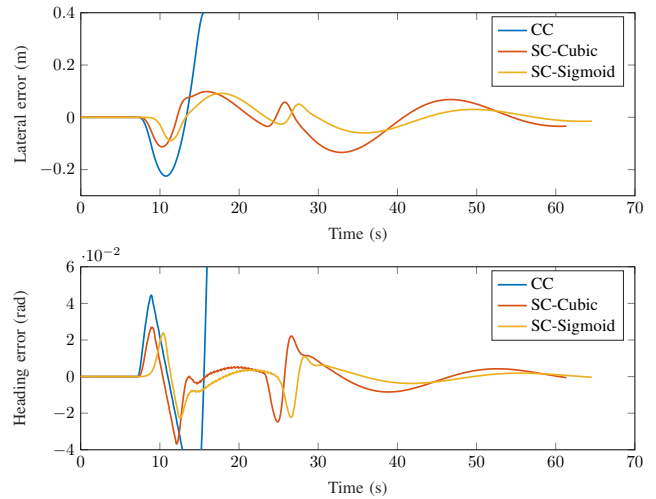


Fig. 6: Error profiles when tracking paths

that the worst controller performance is obtained for the case of the CC paths.

Figure 7 shows the steering angle acceleration request, which corresponds to the output of the PID controller. The request is shown for both the SC-Cubic and SC-Sigmoid paths, the CC path is not shown as it is unstable. It can be seen that the control action is significantly lower in the case of the SC-Sigmoid path, indicating that the steering reference is easier to follow.

The lateral acceleration and jerk (acceleration rate) experienced by the vehicle are related to passenger comfort. In Figure 8, the lateral accelerations are shown for a vehicle which follows the reference steering profiles, without feedback from the lateral and heading errors. It can be seen that the lateral acceleration of the CC paths has large jerk values, which result from an aggressive steering actuation. Both the SC-Cubic and SC-Sigmoid steering profiles achieve smoother lateral acceleration profiles.

The proposed SC paths show a performance improvement, with the SC-Sigmoid path performing slightly better than the

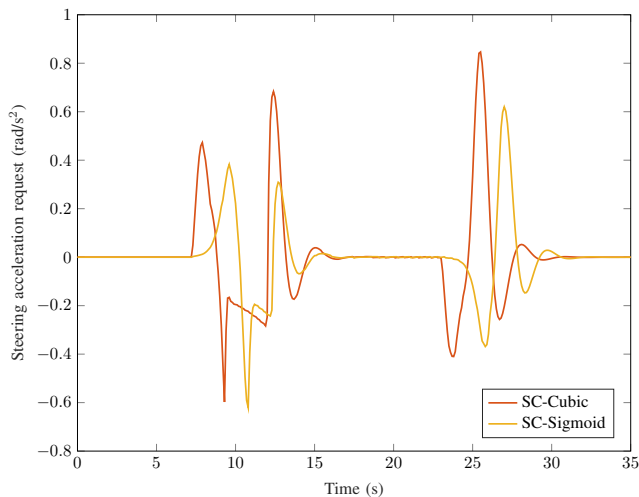


Fig. 7: Controller steering angle acceleration request when tracking a path

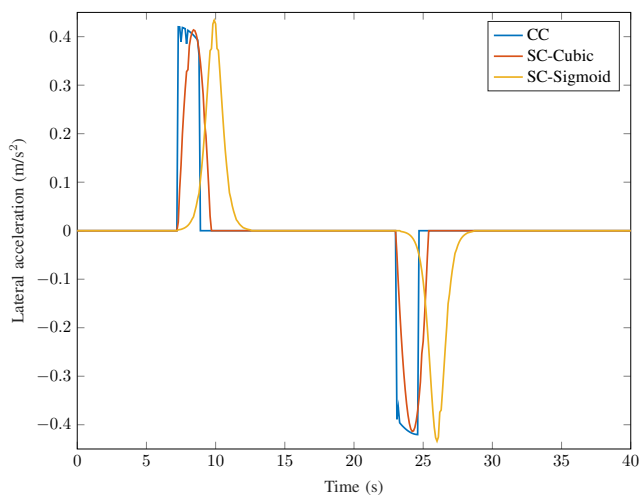


Fig. 8: Lateral acceleration when tracking a path

SC-Cubic path. Although being both sharpness continuous, the SC-Sigmoid path presents a smoother steering profile when compared against the SC-Cubic path, which results in a better tracking of the steering reference, and consequently on a better path tracking performance.

VII. CONCLUSIONS

In this paper, we presented the concept of SC paths. The proposed paths have the characteristic of respecting not only the maximum steering angle constraints, but also maximum steering rate and acceleration constraints. These properties are of importance as they ease the low-level controller task, by taking into account important steering actuator limitations, and consequently providing feasible to track paths. Furthermore, these paths present an higher degree of smoothness, which improves the driving comfort and reduces actuator effort.

As future work, one could extend this approach by allowing the SC paths to handle more possible cases besides that

of generating a path from a combination of two SC turns connected by a line segment. This would allow the SC paths to be able to connect configurations that lie close together.

It is important to evaluate the path tracking performance of a controller using these type of paths on a real system. In this paper, the controllers used were simplified ones, which are not often used in real systems that must achieve high performance. It can be argued that more complex controller approaches, such as Model Predictive Controllers (MPC) will not have significant performance changes when using the proposed paths. Nonetheless, alternative controllers could be designed such that they take full advantage of the properties of the path, without requiring the computational effort of MPC techniques.

This work can also be extended into time optimal trajectory planning. Currently the SC paths assume a constant velocity, however, the velocity profile could be optimized, such that the vehicle can perform the path in a time optimal way, while still obeying steering constraints. Moreover, instead of applying an *a posteriori* velocity profile optimization, a different curvature profile could be optimized with respect to time, and abiding by the steering constraints.

REFERENCES

- [1] M. Buehler *et al.*, eds., The DARPA urban challenge: autonomous vehicles in city traffic. Vol. 56. Springer, 2009.
- [2] H. Choset *et al.*, Principles of robot motion: theory, algorithms, and implementation. MIT press, 2005.
- [3] Y. Kuwata *et al.*, "Real-time motion planning with applications to autonomous urban driving" IEEE Transactions on Control Systems Technology 17, no. 5 (2009): 1105-1118.
- [4] S. Karaman *et al.*, "Anytime motion planning using the RRT," in Robotics and Automation (ICRA), 2011 IEEE Int. Conf. on, pp. 1478-1483. IEEE, 2011.
- [5] T. Shima *et al.*, "Multiple task assignments for cooperating uninhabited aerial vehicles using genetic algorithms" Computers & Operations Research 33, no. 11 (2006): 3252-3269.
- [6] D. Dolgov *et al.*, "Path planning for autonomous vehicles in unknown semi-structured environments" The International Journal of Robotics Research 29, no. 5 (2010): 485-501.
- [7] L. E. Dubins, "On curves of minimal length with a constraint on average curvature, and with prescribed initial and terminal positions and tangents" American Journal of mathematics 79, no. 3 (1957): 497-516.
- [8] J. Reeds and L. Shepp, "Optimal paths for a car that goes both forwards and backwards" Pacific journal of mathematics 145, no. 2 (1990): 367-393.
- [9] T. Fraichard and A. Scheuer, "From Reeds and Shepp's to continuous-curvature paths" IEEE Transactions on Robotics 20, no. 6 (2004): 1025-1035.
- [10] P. F. Lima *et al.*, "Clothoid-based model predictive control for autonomous driving" In Control Conference (ECC), 2015 European, pp. 2983-2990. IEEE, 2015.
- [11] B. Nagy and A. Kelly, "Trajectory generation for car-like robots using cubic curvature polynomials" Field and Service Robots 11 (2001).
- [12] G. Parlangeli and G. Indiveri, "Dubins inspired 2D smooth paths with bounded curvature and curvature derivative" IFAC Proceedings Volumes 43, no. 16 (2010): 252-257.
- [13] A. Scheuer and T. Fraichard, "Continuous-curvature path planning for car-like vehicles" In Intelligent Robots and Systems, 1997. IROS'97., Proceedings of the 1997 IEEE/RSJ International Conference on, vol. 2, pp. 997-1003. IEEE, 1997.
- [14] A. Piazzini *et al.*, "Smooth Path Generation for Wheeled Mobile Robots Using η^3 -Splines" In Motion Control. InTech, 2010.